**Proceedings of the ASME 2018 International Design Engineering Technical Conferences and Computers and Information in Engineering Conference**
**IDETC2018**
**August 26-29, 2018, Quebec City, Quebec, Canada**

**DETC2018-85929**

# HIGHER-ORDER MULTIPLE SCALES ANALYSIS OF WEAKLY NONLINEAR LATTICES WITH IMPLICATIONS FOR DIRECTIONAL STABILITY

**Matthew D. Fronk**
Graduate Student
School of Mechanical Engineering
Georgia Institute of Technology
Atlanta, GA 30332, USA
mfronk3@gatech.edu

**Michael J. Leamy***
Professor
School of Mechanical Engineering
Georgia Institute of Technology
Atlanta, GA 30332, USA
michael.leamy@me.gatech.edu

## ABSTRACT
Recent focus has been given to nonlinear periodic structures for their ability to filter, guide, and block elastic and acoustic waves as a function of their amplitude. In particular, two-dimensional (2-D) nonlinear structures possess amplitude-dependent *directional* bandgaps. However, little attention has been given to the stability of plane waves along different directions in these structures. This study analyzes a 2-D monoatomic shear lattice composed of discrete masses, linear springs, quadratic and cubic nonlinear springs, and linear viscous dampers. A local stability analysis informed by perturbation results retained through the second order suggests that different directions become unstable at different amplitudes in an otherwise symmetrical lattice. Simulations of the lattice's equation of motion subjected to both line and point forcing are consistent with the local stability results: waves with large amplitudes have spectral growth that differs appreciably at different angles. The results of this analysis could have implications for encryption strategies and damage detection.

**Keywords**: 2-D periodic structures, nonlinear wave propagation, stability, Method of Multiple Scales

## 1 INTRODUCTION
Periodic structures have been an active area of research, in part due to their inherent filtering capabilities, which inspires applications such as acoustic filters [1, 2], waveguides [3-5], and diodes [6, 7]. Some of the earliest studies of linear periodic structures dates back to the work of Brillouin [8] and Kittel [9], that analyzed elastic and electric monoatomic and diatomic lattices. Significant advancements in the analysis of waves in elastic periodic media stemmed from Mead *et al*. that characterizes plane wave propagation in periodic plates [10, 11].

Prior studies have employed perturbation techniques to analyze wave propagation in nonlinear periodic systems. Vakakis and King [12] reported amplitude-dependent propagation and attenuation zones in nonlinear periodic structures by application of multiple scales in space and time. Narisetti *et al*. [13] as well as Manktelow *et al.* [14] studied 2-D monoatomic and diatomic lattices with an emphasis on obtaining and numerically verifying amplitude-dependent dispersion shifts. However, these asymptotic techniques stop at the 1st order, thereby limiting the information about wave propagation in these systems since higher-order analysis has been shown to reveal the existence of unstable fixed points [15].

Many prior analyses have identified angular-dependent phenomena in two-dimensional periodic structures. Majunath *et al.* [16] studied the propagation of impacts in 2-D granular media: angular dependence was reported for the transmitted force amplitude and induced propagation angle for layers below the impact. Directional bandgaps have been presented in 2-D periodic structures including auxetic and chiral lattices [17, 18] as well as plates with truss-like cores [19]. Thus, compared to their 1-D counterpart, 2-D structures filter directions in addition to frequencies of propagation. Cleavage fracture was found to occur in preferential directions in silicon whereas other directions exhibit relaxation of the surrounding atoms and large lattice trapping [20]. To the author's knowledge, what remains to be reported in two-dimensional periodic structures is the directional stability of plane waves: a directional-dependence on

* Address all correspondence to this author.



Copyright © 2018 by ASME

the amplitude at which the plane wave solution breaks down. While numerous studies have examined the stability of waves in nonlinear lattice structures, there is a lack of analysis on the stability of plane waves, *i.e.* waves of infinite temporal and spatial extent that possess a fundamental frequency and (potentially) higher harmonics of that frequency. By contrast, studies have examined waveforms such as solitary waves [21], gap solitons [22] and discrete breathers [23].

This study conducts higher-order multiple scales analysis on the equations of motion governing a 2-D monoatomic lattice with weak quadratic and cubic nonlinearities. Results retained through the second order inform a local stability analysis on the wave's amplitude, yielding direction-dependent stability behavior. Direct numerical simulations qualitatively confirm the study's findings.

## 2 SYSTEM DESCRIPTION

The system considered in this analysis is a 2-D monoatomic shear lattice (see Fig. 1): a unit cell composed of a single mass is repeated in two orthogonal directions and only out-of-plane displacements are permitted. Each mass is coupled to its four nearest neighbors via a linear spring, linear damper, and quadratic and cubic nonlinear springs.

**Figure 1. Unit cell of the 2-D monoatomic lattice**

The equations of motion governing the lattice are

$$\begin{aligned} m\ddot{z}_{j,k} + k_{1x}\left(z_{j,k} - z_{j-1,k} - z_{j+1,k}\right) + k_{1y}\left(z_{j,k} - z_{j,k-1} - z_{j,k+1}\right) \\ +\varepsilon k_{2x}\left(z_{j,k} - z_{j-1,k}\right)^2 + \varepsilon k_{2x}\left(z_{j,k} - z_{j+1,k}\right)^2 \\ +\varepsilon k_{2y}\left(z_{j,k} - z_{j,k-1}\right)^2 + \varepsilon k_{2y}\left(z_{j,k} - z_{j,k+1}\right)^2 \\ +\varepsilon k_{3x}\left(z_{j,k} - z_{j-1,k}\right)^3 + \varepsilon k_{3x}\left(z_{j,k} - z_{j+1,k}\right)^3 \\ +\varepsilon k_{3y}\left(z_{j,k} - z_{j,k-1}\right)^3 + \varepsilon k_{2y}\left(z_{j,k} - z_{j,k+1}\right)^3 \\ +\varepsilon c_x\left(\dot{z}_{j,k} - \dot{z}_{j-1,k} - \dot{z}_{j+1,k}\right) \\ +\varepsilon c_y\left(\dot{z}_{j,k} - \dot{z}_{j,k-1} - \dot{z}_{j,k+1}\right) = 0 \end{aligned} \quad (1)$$

where $z_{j,k}$ denotes the out-of-plane displacement of the mass located at $(j,k)$, $m$ the mass, and $k_{1x}, k_{1y}$ the linear stiffness in the $x$ and y directions, respectively. The same naming convention applies to the damping coefficients $(c_x, c_y)$, quadratic stiffnesses $(k_{2x}, k_{2y})$, and cubic stiffnesses $(k_{3x}, k_{3y})$. The small parameter $\varepsilon$ is employed as a bookkeeping device. Linear restoring forces could arise from a non-zero pretension (*e.g.,* from a membrane-like material) and must be considered in order to apply perturbation techniques to this weakly nonlinear system. In contrast, other recent studies of analogous discrete systems neglect pretension, giving rise to strongly nonlinear equations of motion governing the transverse motion of particles [24].

## 3 ANALYSIS APPROACH

If the bookkeeping term is small ($\varepsilon \ll 1$), then the nonlinear interactions are weak and the Method of Multiple Scales (MMS) [25] can readily be applied to Eq. (1). This analysis technique introduces various time scales at which the system evolves

$$T_0 = t, T_1 = \varepsilon t, \dots, T_n = \varepsilon^n t \quad (2)$$

It follows that time derivatives can be expressed as

$$\left(\dot{\ }\right) = D_0(\ ) + \varepsilon D_1(\ ) + \cdots + \varepsilon^n D_n(\ ) \quad (3)$$

and

$$\begin{aligned} \left(\ddot{\ }\right) = D_0^2(\ ) + 2\varepsilon D_0 D_1(\ ) + \varepsilon^2 D_1^2(\ ) + \\ 2\varepsilon^2 D_0 D_2(\ ) + O(\varepsilon^3) \end{aligned} \quad (4)$$

where $D_n(\ )$ denotes differentiation with respect to $T_n$. Additionally, a series solution is imposed of the form

$$z_{j,k} = z_{j,k}^{(0)} + \varepsilon z_{j,k}^{(1)} + \cdots + \varepsilon^n z_{j,k}^{(n)} \quad (5)$$

The equation governing the 0th order is,

$$\begin{aligned} mD_0^2 z_{j,k}^{(0)} + k_{1x}\left(z_{j,k}^{(0)} - z_{j-1,k}^{(0)} - z_{j+1,k}^{(0)}\right) \\ +k_{1y}\left(z_{j,k}^{(0)} - z_{j,k-1}^{(0)} - z_{j,k+1}^{(0)}\right) = 0 \end{aligned} \quad (6)$$

which is known to admit a Bloch wave

$$z_{j,k}^{(0)} = \frac{1}{2} A e^{i\omega_0 T_0} e^{-i\mu_x j} e^{-i\mu_y k} + c.c. \quad (7)$$

where $A$ denotes the complex wave amplitude, $\omega_0$ and $\mu$ denote the fundamental temporal and spatial frequencies, respectively, and $c.c.$ denotes the complex conjugate of all preceding terms. $A(T_1, T_2, \dots, T_n)$ can be expressed in polar form

$$A = \alpha e^{i\beta} \quad (8)$$

where $\alpha = \alpha(T_1, T_2, \dots T_n)$ and $\beta = \beta(T_1, T_2, \dots, T_n)$. Substitution of the Bloch waveform into the 0th-order governing equation yields the linear dispersion relationship,

$$\omega_0 = \sqrt{\frac{2k_{1x}}{m}(1 - \cos\mu_x) + \frac{2k_{1y}}{m}\left(1 - \cos\mu_y\right)} \quad (9)$$

Next, updating the 1st-order equation with the 0th-order results yields

$$\begin{aligned} mD_0^2 z_{j,k}^{(1)} + k_{1x}\left(z_{j,k}^{(1)} - z_{j-1,k}^{(1)} - z_{j+1,k}^{(1)}\right) \\ +k_{1y}\left(z_{j,k}^{(1)} - z_{j,k-1}^{(1)} - z_{j,k+1}^{(1)}\right) = f_{secular} + f_{nonsecular} \end{aligned} \quad (10)$$

It is apparent that the left-hand side of Eq. (10) resembles that of the 0th-order equation. Furthermore, the right-hand side contains both secular forcing terms (*i.e.,* those containing $e^{i\omega_0 T_0} e^{-i\mu_x j} e^{-i\mu_y k}$) and nonsecular forcing terms (*i.e.,* those containing $e^{ni\omega_0 T_0} e^{-ni\,\mu_x j} e^{-ni\mu_y k}, n = 2,3$). To preserve the


Copyright © 2018 by ASME

convergence of the series expansion in Eq. (5), all secular terms must be removed, which can be accomplished by a unique choice of $D_1\alpha$ and $D_1\beta$

$$D_1\alpha = -\gamma_{xy}\alpha \tag{11}$$

$$D_1\beta = \delta_{xy}\alpha^2 \tag{12}$$

where $\gamma_{xy}$ and $\delta_{xy}$ can be expressed in terms of the lattice parameters in Eq. (1) as well as $\omega_0$ and $\mu$.

With only nonsecular terms remaining in Eq. (10), the 1st-order solution requires only a particular solution,

$$z_{j,k}^{(1)} = \frac{1}{2}B_1 e^{2i\omega_0 T_0} e^{-2i\mu_x j} e^{-2i\mu_y k} + \frac{1}{2}C_1 e^{3i\omega_0 T_0} e^{-3i\mu_x j} e^{-3i\mu_y k} + c.c. \tag{13}$$

where the coefficients can be solved for algebraically via the method of undetermined coefficients.

Analysis at the second order follows a similar approach. Removal of secular terms determines $D_2\alpha$ and $D_2\beta$

$$D_2\alpha = \phi_{xy}\alpha^5 + \xi_{xy}\alpha^3 \tag{14}$$

$$D_2\beta = \mathrm{X}_{xy}\alpha^4 + \Upsilon_{xy}\alpha^2 + \mathrm{Z}_{\mathrm{xy}} \tag{15}$$

where $\phi_{xy}, \xi_{xy}, \mathrm{X}_{xy}, \Upsilon_{xy}$, and $\mathrm{Z}_{\mathrm{xy}}$ can be expressed in terms of the lattice parameters in Fig. 1 as well as $\omega_0$ and $\mu$. The nonsecular forcing terms generates a second order particular solution of the form

$$z_{j,k}^{(2)} = \frac{1}{2}B_2 e^{2i\omega_0 T_0} e^{-2i\mu_x j} e^{-2i\mu_y k} + \frac{1}{2}C_2 e^{3i\omega_0 T_0} e^{-3i\mu_x j} e^{-3i\mu_y k} + \frac{1}{2}E_2 e^{4i\omega_0 T_0} e^{-4i\mu_x j} e^{-4i\mu_y k} + \frac{1}{2}F_2 e^{5i\omega_0 T_0} e^{-5i\mu_x j} e^{-5i\mu_y k} + c.c. \tag{16}$$

The MMS results from both the first and second order reveal a unique multi-harmonic profile that this structure supports. Prior studies of 1-D systems confirm that the addition of terms from the series solution converges to an invariant waveform: a distribution of harmonic energy that propagates without dispersing for all space and time [15]. Numerical validation of waveform invariance in this 2-D lattice will be investigated in future work.

## 4 LOCAL STABILITY ANALYSIS

It is of practical interest to know the stability of wave propagation in these nonlinear systems: under what conditions will a plane wave cease to propagate at its prescribed solution form? Amplitude can be expected to play a critical role in determining the stability of the wave propagation solutions found. For sufficiently large amplitudes, nonlinear interactions dominate and plane wave propagation may break-down as the medium can no longer support the waveform injected into it (that assumes weak nonlinearities). Such knowledge could limit the operational amplitude range of devices that exploit nonlinear effects (*e.g.,* bandgap shifting). Less intuitive is the influence of propagation *direction* on stability, especially for a symmetrical lattice. However, a local stability analysis indeed reveals fixed-points that vary with propagation angle, a finding, to the authors' knowledge, that has yet to be reported in discrete nonlinear periodic structures.

Reconstituting the 0th order amplitude to the original time scale yields an evolution equation

$$\dot{\alpha} = \varepsilon D_1(\alpha) + \varepsilon^2 D_2(\alpha) \tag{17}$$

Denoting the fixed point solutions as $\alpha^*$, the stability of each fixed point is assessed through a local analysis by computing its associated $\lambda$ value

$$\lambda \equiv \frac{d}{d\alpha}\dot{\alpha}|_{\alpha^*} \tag{18}$$

where $\lambda > 0$ implies instability, $\lambda < 0$ stability, and $\lambda = 0$ neutral stability.

Whether truncated at the 1st or 2nd order, the stable fixed point $\alpha^* = 0$ arises from the analysis. Such solution indicates that small amplitude waves decay due to damping in the structure. Higher-order (*i.e.,* $O(\varepsilon^2)$) terms in the reconstituted evolution equation reveal unstable non-zero fixed points ($\alpha^* = \alpha^*_{NZ}$). Thus, amplitudes greater than these critical values grow unboundedly whereas amplitudes less than these critical values decay to the attractor at $\alpha^* = 0$.

While not immediately apparent when examining the MMS results, the unstable fixed points in the symmetric system exhibit strong angular dependence. Figure 2 plots the unstable fixed points as a function of $\theta$, the angle of the plane wave in the lattice. Note that, while symmetric parameters are used, there is still the indication of *directional stability* in the system: stability increases as the angle increases since higher $\alpha^*$ values imply greater stability.

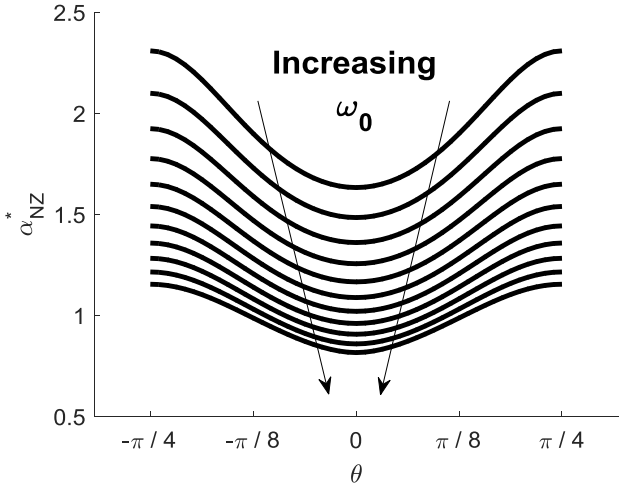


**Figure 2. Unstable fixed points evaluated as a function of propagation angle at various frequencies, exhibiting more stability as the angle departs from $= \mathbf{0}: \boldsymbol{m} = \mathbf{1}, \boldsymbol{k_{1,x}} = \mathbf{1}, \boldsymbol{k_{1,y}} = \mathbf{1}, \boldsymbol{k_{2,x}} = \mathbf{1}, \boldsymbol{k_{2,y}} = \mathbf{1}, \boldsymbol{k_{3,x}} = \mathbf{1}, \boldsymbol{k_{3,y}} = \mathbf{1}, \boldsymbol{c_x} = \mathbf{0.1}, \boldsymbol{c_y} = \mathbf{0.1}$**

Figure 3 displays the basins of attraction for a symmetrical lattice with plane waves along different angles, $\theta$, and initial amplitudes, $\alpha_0$. Note that $\alpha_0$ values above the threshold marked by the black line propagate in an unstable manner whereas $\alpha_0$ values below this threshold propagate in a stable manner. The black line is computed from the local stability analysis while the colored points are found from numerically integrating Eq. (17) and identifying, based on the rate of change of the amplitude, if


Copyright © 2018 by ASME

the plane wave propagated stably. Unstable waves possess amplitudes that grow unboundedly whereas stable waves decay to zero due to the presence of damping. Again, note the directional dependence of stability. It is clear that for some amplitudes, *e.g.* $\alpha_0 = 1.5$, the wave propagates in a stable manner along the 45 degree direction, but in an unstable manner along the 0 degree direction.

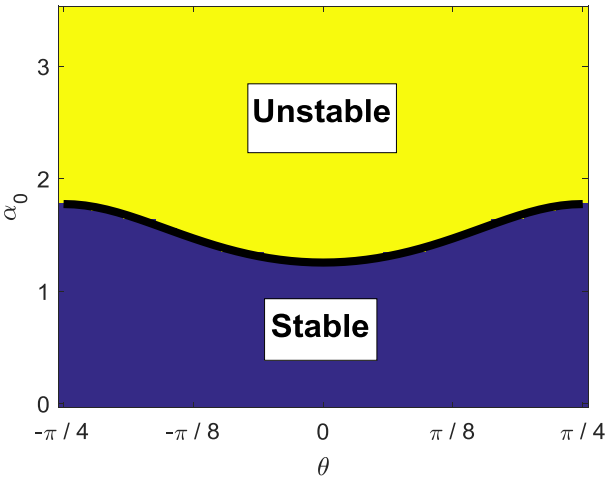


**Figure 3. Basins of attraction for the 2-D lattice. Amplitudes grow unboundedly when greater than directionally-dependent critical values. Otherwise, amplitudes decay to the attractor at $\boldsymbol{\alpha^* = 0}$: $\boldsymbol{m = 1, k_{1,x} = 1, k_{1,y} = 1, k_{2,x} = 1, k_{2,y} = 1, k_{3,x} = 1, k_{3,y} = 1, c_x = 0.1, c_y = 0.1, \omega_0 = 1.3}$**

Similar to the findings in [15], the fixed points from the local stability analysis cannot be expected to accurately predict the true threshold for instability in this system. This conclusion stems from the weak nonlinearity assumption intrinsic to the perturbation analysis: the fixed points indicating a loss of stability are large enough to violate this assumption. Defining the dimensionless strength of the cubic nonlinearity as $\Pi_3 = \varepsilon k_{3x} {\alpha^*_{NZ}}^2 / k_{1x}$, the fixed point that gives the weakest nonlinearity is $\Pi_{3,\min} = 0.667$, well above the conservative limit of 0.1. However, the MMS results do accurately convey that, as supported by the results of numerical simulations presented in the following section, there is directional stability of plane waves in these lattices.

## 5 NUMERICAL STABILITY RESULTS

To investigate the findings of the local stability analysis, direct numerical integration of Eq. (1) is performed at varying wave amplitudes and angles. Large structures (~150 x 150 unit cells) are simulated and viscous dampers with coefficients that increase at a cubic rate outward are added near the boundary to suppress reflections. Harmonic displacements of the form $x(j,k,t) = \alpha \cos \omega t$ are applied to the lattice at either a point or along a line. Clearly, point forcing generates waves along all directions simultaneously whereas line forcing generates waves along prescribed directions. Recall that waves generated by point forcing undergo geometric spreading of their amplitude because of energy conservation. Instability is defined herein as a significant deviation from the expected multiharmonic solution.

Fast Fourier Transforms (FFT's) are computed over time for various unit cells near the forcing location. With this information, the energy $E$ within a frequency band $\Omega_1$ to $\Omega_2$ can be calculated as

$$E = \int_{\Omega_1}^{\Omega_2} |Z(\Omega)|^2 d\Omega \tag{19}$$

where $Z(\Omega)$ is the complex coefficient of the FFT at a given frequency. Using Eq. (19), instabilities can be detected when an appreciable amount of energy falls outside of a narrowband region centered about the forcing frequency. Accordingly, $E_\delta$ can be introduced

$$E_\delta = 1 - \frac{1}{E_{total}} \int_{\omega-\Delta}^{\omega+\Delta} |Z(\Omega)|^2 d\Omega \tag{20}$$

where $E_{total}$ denotes the total spectral energy of the unit cell and $2\Delta$ denotes a small bandwidth centered about the forcing frequency $\omega$.

Figure 4 presents the results of applying a high-amplitude harmonic displacement to the center of a symmetric lattice. The energy outside of the fundamental (forcing) frequency, $E_\delta$, is computed and displayed at each point in the 20 x 20 square region around the center. Black lines represent displacement contours. For a wave that propagates nearly uniformly outward (*i.e.* no beaming, as is known to occur at high frequencies) spectral content differs drastically along different angles far away from the source. The FFT's at two separate locations reveal that propagation along the $x$-direction breaks down from its original fundamental frequency into incommensurate frequencies not predicted by the perturbation analysis, whereas the 45-degree direction retains nearly all the signal information from the point forcing.

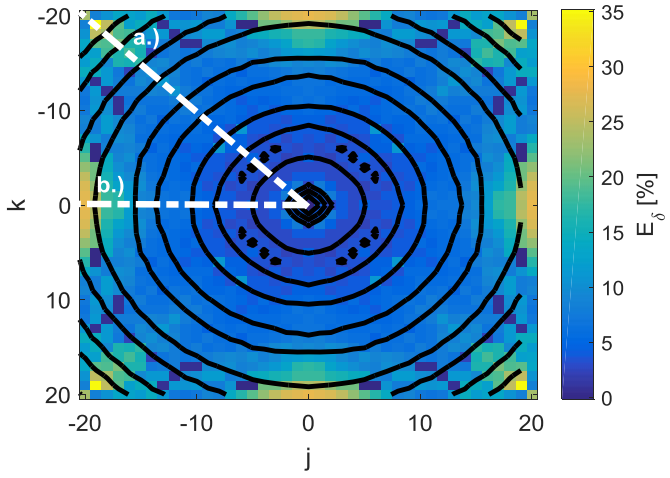



Copyright © 2018 by ASME

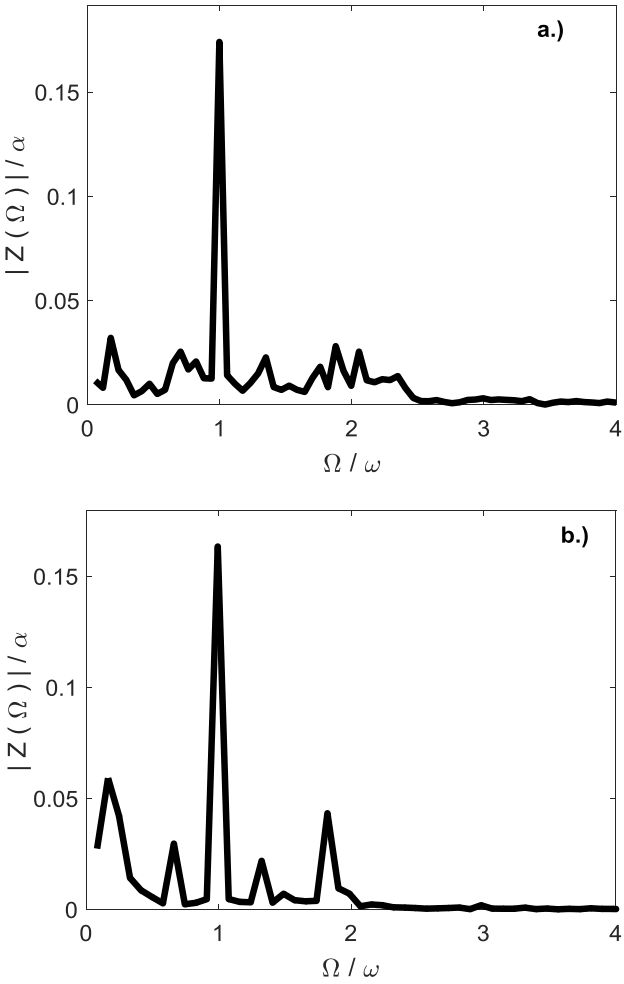


**Figure 4. Point forcing of a lattice at its center. Spectral energy outside of the narrow forcing frequency band varies with direction and is highest at $\theta = 45^o$, consistent with perturbation theory. Stable spectral content at $\theta = 0^o$ (a.) is compared to unstable spectral content at $\theta = 45^o$ (b.), : $m = 1, k_{1,x} = 1, k_{1,y} = 1, k_{2,x} = 0, k_{2,y} = 0, k_{3,x} = 1, k_{3,y} = 1, c_x = 0, c_y = 0, \omega = 1.3, \alpha = 2.7$**

High amplitude line forcing is applied to the system in Fig. 5, producing propagation along the $x$-direction (a.) and 45 degree direction (b.). Visual comparison of the displacements for both cases clearly indicates that the 45 degree direction propagates in a stable manner whereas the $x$-direction does not, consistent with both the numerical results of point forcing and the MMS results.

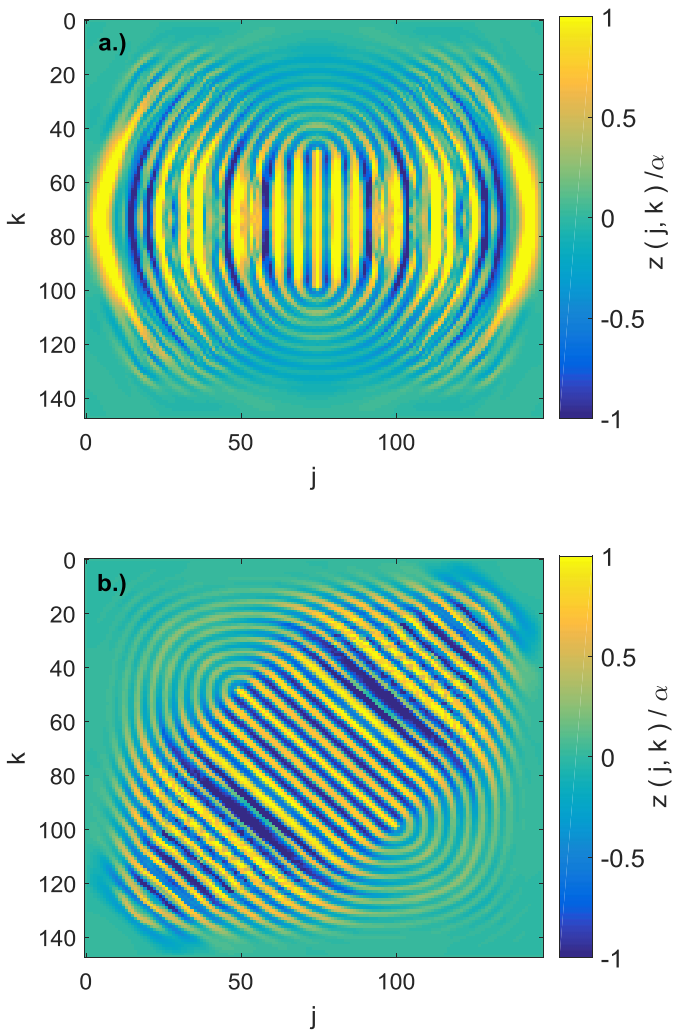


**Figure 5. Line forcing of lattice at high amplitudes for $\theta = 0^o$ (a.) as compared to $\theta = 45^o$ (b.): $m = 1, k_{1,x} = 1, k_{1,y} = 1, k_{2,x} = 0, k_{2,y} = 0, k_{3,x} = 1, k_{3,y} = 1, c_x = 0, c_y = 0, \omega = 1.3, \alpha = 0.9$ a.) $\theta = 0^o$ and b.) $\theta = 45^o$**

Figure 6 depicts the evolution of temporal FFT's over space for the simulations presented in Fig. 5. The range is the number of unit cells (perpendicular to the wavefront) from the location of the center of the line of forcing. Note the consistency with the point forcing results in Fig. 2: spectral content distorts significantly for $\theta = 0^o$ as compared to $\theta = 45^o$. Unlike the point forcing simulation, there is no geometric spreading of amplitude, making line forcing studies useful for identifying the exact amplitude threshold for instability as $\theta$ is varied, which will be done in future work.


Copyright © 2018 by ASME

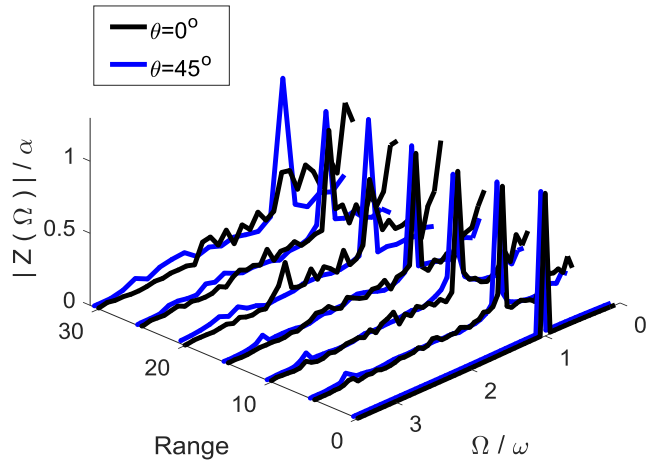


**Figure 6. Spatial evolution of temporal FFT's for a lattice subjected to line forcing. Significant growth of incommensurate frequencies occurs for propagation along $\boldsymbol{\theta = 45^o}$ whereas a stable generation of harmonics occurs for $\boldsymbol{\theta = 0^o}$ . (b.) $\boldsymbol{m = 1, k_{1,x} = 1, k_{1,y} = 1, k_{2,x} = 0, k_{2,y} = 0, k_{3,x} = 1, k_{3,y} = 1, c_x = 0, c_y = 0, \omega = 1.3, \alpha = 0.9}$**

Figure 7 compares $E_\delta$ as a function of the wave's range for unit cells along $\theta = 0^o$ and $45^o$. Note that energy rapidly distributes outside of the forcing frequency band for $\theta = 0^o$ and remains relatively centered around the forcing frequency band for $\theta = 45^o$.

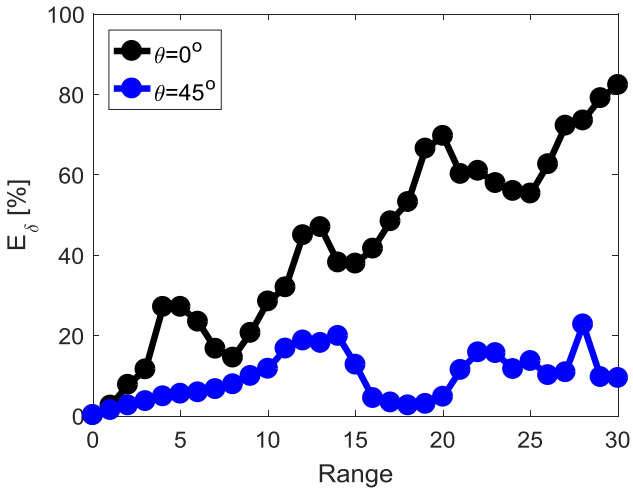


**Figure 7. Spatial evolution of spectral energy for a lattice subjected to line forcing. Energy outside the narrow forcing frequency band is measurably higher along $\boldsymbol{\theta = 45^o}$ than $\boldsymbol{\theta = 0^o}$: $\boldsymbol{m = 1, k_{1,x} = 1, k_{1,y} = 1, k_{2,x} = 0, k_{2,y} = 0, k_{3,x} = 1, k_{3,y} = 1, c_x = 0, c_y = 0, \omega = 1.3, \alpha = 0.9}$**

Continuous structures do not lose stability at different rates along different directions. Thus, this finding illustrates that discrete media leads to novel dynamical behavior in symmetric materials that could inspire new technology. For example, Fig. 8 proposes a new method for spatially encrypting data, in which the phasing between transducers produces a stable plane wave only when the correct passcode is entered. Otherwise, an unstable wave generates incommensurate frequencies and information stored at the fundamental frequency is unreadable.

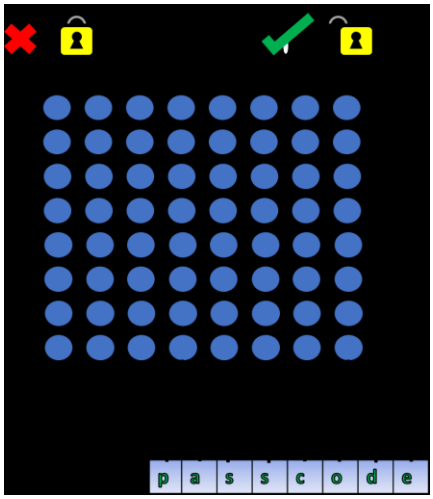


**Figure 8. Encryption of information by setting the phasing between transducers to generate stable plane waves only when the correct passcode is entered.**

Orientation of cracks in structures such as bridges, buildings, and aircraft could be identified in a novel, low power manner. Figure 9 depicts a transducer array mounted on a structure with a crack. Signals from the transducers reveal if the crack is oriented closer to $45^o$ or $0^o$ by simply examining the presence or absence of incommensurate frequencies. Information about crack orientation may be critical for assessing the threat the crack poses to the structure.

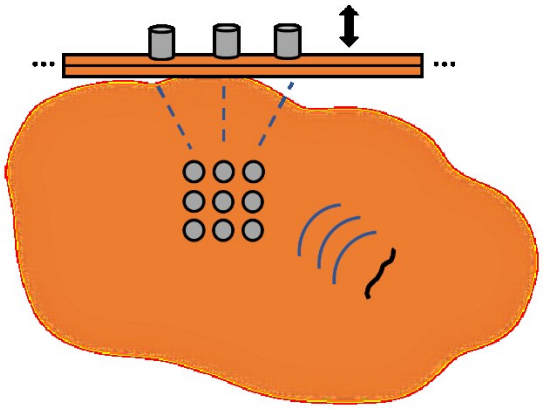

**Figure 9. Orientation of cracks can be detected by examining the presence (or absence) of incommensurate frequencies in a transducer array.**


Copyright © 2018 by ASME

## 6 CONCLUDING REMARKS

A 2-D nonlinear monoatomic shear lattice was analyzed using higher-order multiple scales analysis. A local stability analysis of the wave's amplitude indicates that propagation along a lattice direction propagates less stably than inclined directions. Numerical simulations of the symmetric lattice's equation of motion, under both point and line forcing, confirm this trend. Such findings could inspire new data encryption and damage detection technologies.

## ACKNOWLEDGEMENTS

The authors would like to thank the National Science Foundation for support of this research under Grant No. (CMMI 1332862).

## REFERENCES

[1] Khelif, A., Deymier, P. A., Djafari-Rouhani, B., Vasseur, J. O., and Dobrzynski, L., 2003, "Two-Dimensional Phononic Crystal with Tunable Narrow Pass Band: Application to a Waveguide with Selective Frequency," Journal of Applied Physics, 94 (3), pp. 1308-1311.

[2] Zhang, P., and To, A. C., 2013, "Broadband Wave Filtering of Bioinspired Hierarchical Phononic Crystal," Applied Physics Letters, 102 (12), pp. 121910.

[3] Sun, J.-H., and Wu, T.-T., 2006, "Propagation of Surface Acoustic Waves through Sharply Bent Two-Dimensional Phononic Crystal Waveguides Using a Finite-Difference Time-Domain Method," Physical Review B, 74 (17), pp. 174305.

[4] Popa, B.-I., and Cummer, S. A., 2014, "Non-Reciprocal and Highly Nonlinear Active Acoustic Metamaterials," Nature Communications, 5 pp. 3398.

[5] Zheng, L.-Y., Tournat, V., and Gusev, V., 2017, "Zero-Frequency and Extremely Slow Elastic Edge Waves in Mechanical Granular Graphene," Extreme Mechanics Letters, 12 pp. 55-64.

[6] Chen, J.-J., Han, X., and Li, G.-Y., 2013, "Asymmetric Lamb Wave Propagation in Phononic Crystal Slabs with Graded Grating," Journal of Applied Physics, 113 (18), pp. 184506.

[7] Li, X.-F., Ni, X., Feng, L., Lu, M.-H., He, C., and Chen, Y.-F., 2011, "Tunable Unidirectional Sound Propagation through a Sonic-Crystal-Based Acoustic Diode," Physical Review Letters, 106 (8), pp. 084301.

[8] Brillouin, L., 2003, *Wave Propagation in Periodic Structures: Electric Filters and Crystal Lattices*, Dover Publications,

[9] Kittel, C., 1971, *Introduction to Solid State Physics*, Wiley,

[10] Mead, D. J., and Parthan, S., 1979, "Free Wave Propagation in Two-Dimensional Periodic Plates," Journal of Sound and Vibration, 64 (3), pp. 325-348.

[11] Mead, D. J., Zhu, D. C., and Bardell, N. S., 1988, "Free Vibration of an Orthogonally Stiffened Flat Plate," Journal of Sound and Vibration, 127 (1), pp. 19-48.

[12] Vakakis, A. F., and King, M. E., 1995, "Nonlinear Wave Transmission in a Monocoupled Elastic Periodic System," The Journal of the Acoustical Society of America, 98 (3), pp. 1534-1546.

[13] Narisetti, R. K., Ruzzene, M., and Leamy, M. J., 2011, "A Perturbation Approach for Analyzing Dispersion and Group Velocities in Two-Dimensional Nonlinear Periodic Lattices," Journal of Vibration and Acoustics, 133 (6), pp. 061020-061020-12.

[14] Manktelow, K. L., Leamy, M. J., and Ruzzene, M., 2014, "Weakly Nonlinear Wave Interactions in Multi-Degree of Freedom Periodic Structures," Wave Motion, 51 (6), pp. 886-904.

[15] Fronk, M. D., and Leamy, M. J., 2017, "Higher-Order Dispersion, Stability, and Waveform Invariance in Nonlinear Monoatomic and Diatomic Systems," Journal of Vibration and Acoustics, 139 (5), pp. 051003-051003-13.

[16] Manjunath, M., Awasthi, A. P., and Geubelle, P. H., 2014, "Plane Wave Propagation in 2d and 3d Monodisperse Periodic Granular Media," Granular Matter, 16 (1), pp. 141-150.

[17] Ruzzene, M., and Scarpa, F., 2005, "Directional and Band-Gap Behavior of Periodic Auxetic Lattices," physica status solidi (b), 242 (3), pp. 665-680.

[18] Spadoni, A., Ruzzene, M., Gonella, S., and Scarpa, F., 2009, "Phononic Properties of Hexagonal Chiral Lattices," Wave Motion, 46 (7), pp. 435-450.

[19] Kohrs, T., and Petersson, B. a. T., 2009, "Wave Beaming and Wave Propagation in Light Weight Plates with Truss-Like Cores," Journal of Sound and Vibration, 321 (1), pp. 137-165.

[20] Pérez, R., and Gumbsch, P., 2000, "Directional Anisotropy in the Cleavage Fracture of Silicon," Physical Review Letters, 84 (23), pp. 5347-5350.

[21] Friesecke, G., and Pego, R. L., 2002, "Solitary Waves on Fpu Lattices: Ii. Linear Implies Nonlinear Stability," Nonlinearity, 15 (4), pp. 1343.

[22] Huang, G., and Hu, B., 1998, "Asymmetric Gap Soliton Modes in Diatomic Lattices with Cubic and Quartic Nonlinearity," Physical Review B, 57 (10), pp. 5746-5757.

[23] Flach, S., and Gorbach, A. V., 2008, "Discrete Breathers — Advances in Theory and Applications," Physics Reports, 467 (1), pp. 1-116.

[24] Gendelman, O. V., Zolotarevskiy, V., Savin, A. V., Bergman, L. A., and Vakakis, A. F., 2016, "Accelerating Oscillatory Fronts in a Nonlinear Sonic Vacuum with Strong Nonlocal Effects," Physical Review E, 93 (3), pp. 032216.

[25] Ali Hasan Nayfeh, D. T. M., 1995, *Nonlinear Oscillations*, John Wiley & Sons, Inc.,


Copyright © 2018 by ASME